Model sensitivity and nonlinear interactions during extreme sea level events in a wide and fast-flowing estuary: the case of the Río de la Plata

Matías G. Dinapoli[(*)(1,2)], Claudia G. Simionato[(1,2,3)] and Diego Moreira[(1,2,3)]

[(1)] Centro de Investigaciones del Mar y la Atmósfera (CIMA/CONICET-UBA)

[(2)] Instituto Franco-Argentino para el Estudio del Clima y sus Impactos (UMI IFAECI/CNRS-CONICET-UBA)

[(3)] Departamento de Ciencias de la Atmósfera y los Océanos, FCEN, Universidad de Buenos Aires, Argentina.

(*) *Corresponding author:*

Intendente Güiraldes 2160 - Ciudad Universitaria

Pabellón II - 2do. Piso

(C1428EGA) Ciudad Autónoma de Buenos Aires - Argentina

Phone: (+54) 11 4787 2693

(+54) 11 4576 3300/09 Ext. 388

Fax: (+54) 11 4788 3572

Email: matias.dinapoli@cima.fcen.uba.ar

Submitted in revision to Natural Hazards and Earth System Sciences

August 15th, 2017

Abstract. The mighty Río de la Plata (RdP) estuary is affected by extreme storm surges generated by persistent and strong south-easterly winds called "Sudestadas", which produce strong floods in densely populated areas of Argentina. Atmospheric models show deficiencies in the forecast of winds during those events what rises up the question of how sensitive model solutions are to wind uncertainties. Here a sensitivity analysis (SA) for a 2-D barotropic application of ROMS_AGRIF ocean model for the forecast of sea surface height (SSH) at the South-Western South Atlantic Continental Shelf with emphasis on the RdP estuary is presented. The SA was performed taking account the linear and quadratic bottom friction coefficients, the wind speed and direction, and the continental discharge. Results indicate that the estuary response is very sensitive and nonlinear to even small changes in wind speed, and moderately sensitive to changes in the runoff. A study of nonlinear interactions between the surge, the tide and the continental discharge shows that those interactions are strong, producing reductions of around 10% in the total SSH. 90% of that interaction is explained by the tide-surge interaction. The main effect of large increments in the runoff is an increment in the setup, but also the associated augment of the mean outflow currents produces notorious deformations in the storm surge and tides. It is concluded that the inclusion of both the tide and the runoff are indispensable for an appropriate prediction of the SSH in the upper and intermediate RdP.

1. Introduction

The area between 30 °S and 45 °S is characterized by one of the highest cyclogenetic activities within the Southern Hemisphere (*e.g.*, Necco, 1982; Sinclair, 1994; Gan and Rao, 1991). Over that area, cyclogenesis events have a mean frequency of around 120 events by year (Gan and Rao, 1991), with higher frequency during winter and spring. These events are associated to atmospheric waves that move along subtropical latitudes of the South Pacific and South American regions (Vera et al., 2002). When cyclones develop over Uruguay, they can yield very strong and persistent south-easterly winds, known as "Sudestadas", with speeds that can easily exceed 15 m s^{-1} (Seluchi, 1995; Seluchi and Saulo, 1996). The coincidence of large or even moderately high tides and the large meteorologically induced surges during those Sudestadas, has historically caused catastrophic floods in the Río de la Plata coasts, threatening and claiming human lives and producing major economic and material damages (D'Onofrio et al., 1999). This phenomenon affects, in particular, the Metropolitan Area of Buenos Aires City (AMBA), site of the Capital of Argentina, located on the upper RdP estuary (Fig. 1). Balay (1961) defined risk water levels over the Tidal Datum of the RdP at the AMBA in 2.50 m for alert, 2.80 m for emergency and 3.20 m for evacuation (Escobar et al., 2004). Since records began in 1905, the maximum water level at AMBA was registered in 1940. Enhanced by strong south-easterly winds, it reached 4.44 m above the Tidal Datum, being the tidal height overcome by 3.18 m (storm surge maximum). More recently, for instance in 1989 and 1993, extreme floods were also experienced at the city. Water levels reached 4.06 m and 3.95 m above the Tidal Datum, being the storm surge maximums of 3.25 m and 2.49 m, respectively (D'Onofrio et al., 1999). Even though the events are not always so extreme, they are frequent, taking place several times per year. It has been suggested that the flooding is mainly due to combination of tides and surge (D'Onofrio et al., 1999), but the nonlinear interactions between them and the effect of the large continental discharge that characterizes this estuary have not been fully studied yet.

In above described context, the need of forecast models for the prediction of sea level height (SSH) and eventually other variables in the region is evident. Currently, in the frame of a collaborative project between the Hydrographic Service of Argentine (SHN) and the Centre for Atmospheric and Oceanic Research (CIMA/CONICET-UBA) the implementation of such a model for the RdP and the adjacent Continental Shelf is being faced. In this sense, the choice of a forecast numerical model is, naturally, strongly dependent on the quality and reliability of its solutions. However, all models are imperfect

abstractions of Nature. Because the discrete nature of the models, the parameterizations and the inaccuracy of the forcing data, numerical solutions always present errors and uncertainties. The errors in forcing data and the uncertainties on the modelling parameters are not independent each other, but can interact in many ways, eventually driving to numeric solutions that might significantly differ of the observations. In this sense, before adopting a particular model for practical applications, it is necessary to determine the sensitivity of model solutions to changes and interactions in the inputs. The usual manner to do this is by means of a Sensitivity Assessment (SA), which investigates the relation between the inputs and the outputs of simulation models (Saltelli et al., 2000). SA allows to know how model's solutions change with the diverse parameterizations, forcings and boundary conditions. In addition, it shows where the model needs improvements contributing to further model development (Norton, 2015) and allows to optimally assemble a regional model through a reduced number of simulations.

In this sense, the first objective of this paper is to perform a SA of a regional application of ROMS_AGRIF model (Regional Ocean Modeling System, http://www.romsagrif.org) specially implemented for the Northern Argentinean Continental Shelf, with focus in the RdP estuary. Besides analyzing the model sensitivity to potential uncertainties in the model parameters, we consider the effect of the errors and spatial resolution of atmospheric models in the area, where the width of the estuary and the associated physical processes (for instance, sea breeze) turns the proper estimation of wind speed and direction in a challenge.

On the other hand, it is known that storm surges can interact with tides altering sea level (*e.g.* Flather, 2001). This aspect has been studied from the theoretical and numerical point of view (*e.g.* Rossiter, 1961; Zhang, 2010; Idier, 2012). Understanding those interactions is important on the development of operational models, to properly choose the forecast strategy (Idier et al., 2012). If the interaction is significant, then the results of either computing the tide and surge together or, for instance, estimating the surge from numerical simulations and the tide empirically, might be significantly different. In addition, for the particular case of mighty RdP (where discharge peaks of up to 90,000 $m^3 s^{-1}$ have been observed), the nonlinear interactions between the surge and the tide with the continental discharge is another aspect of potential relevance for the prediction of sea level (*e.g.*, Maskell et al., 2014; Klerk et al., 2015). Even though previous studies have shown that the tide interacts with the runoff in the RdP (Luz Clara Tejedor et al., 2014), the interaction between the surge and the discharge has not been evaluated yet. Therefore, this work is complemented with a set of process oriented numerical simulations conceived to analyse the nonlinear interactions between the surge, the tide and the continental discharge in the RdP.

The results of this work constitute a basic and necessary input for the implementation of an operational model for the forecast of SSH in the economically, socially and ecologically important region of the RdP estuary.

2. Study area

The RdP (Fig. 1) is one of the largest estuaries in the world (Shiklomanov, 1998). It is formed by the confluence of the Paraná and Uruguay rivers, which form the second largest basin of South America, after the Amazon (Meccia et al., 2009). The RdP is located at approximately at 35 °S on the eastern coast of southern South America, and has a funnel shape, with a length of approximately 300 km and breadths of 40 km at its head end and 220 km at its mouth (Meccia et al., 2009). The

upper and intermediate estuary has a mean depth of only 10 m, that rapidly increase downstream the Barra del Indio shoal (Fig. 1, Balay, 1961).

The RdP has a very large continental discharge, with a mean value of around 22,000 $m^3 s^{-1}$, ranking 5th worldwide in water discharge (Farmiñan et al., 1999). Nevertheless, the runoff presents large variability associated to El Niño - Southern Oscillation cycles (ENSO, Robertson and Mechoso, 1998) with peaks as high as 90,000 $m^3 s^{-1}$ and as low as less than 8,000 $m^3 s^{-1}$ (Jaime et al., 2002).

The RdP impacts the nutrient, sediment, carbon and freshwater budgets of the South Atlantic Ocean (*e.g.*, Framiñan et al., 1999; Strub et al., 2015), affects the hydrography of the adjacent Continental Shelf, impacts important coastal fisheries, and influences coastal dynamics up to more than 400 km north on the Brazilian shelf (*e.g.*, Campos et al., 1999; Framiñan et al., 1999; Piola et al., 2000).

The RdP is of large social, ecological and economic importance for the countries along its margins, Argentina and Uruguay. The capital cities (Buenos Aires and Montevideo) and the main industrial poles and resorts are located on its margins. The estuary is an area of spawning and nursery for a conglomerate of coastal species (*e.g.*, Acha and Macchi, 2000; Jaureguizar et al., 2003b, 2008). The RdP has several important navigation channels to reach the northern part of Argentina so as Paraguay, which are important for the economy of the countries and demand regular dredging. Finally, the estuary is an important amusement zone and the main source of drinking water for the millions of inhabitants in the region. Being the most developed basin of southern South America, the RdP is strongly impacted by anthropogenic actions.

3. Input data and methods

3.1. ROMS_AGRIF regionalization to the RdP and the adjacent shelf

ROMS (Regional Ocean Modeling System, https://www.myroms.org) is a numerical model developed by Shchepetkin and McWilliams (2005). It is programmed to simulate physical, biogeochemical, biooptic, sedimentological and sea ice applications. This model has been implemented in several areas including in the Patagonian Continental Shelf (*e.g.*, Tonini and Palma, 2009; Combes and Matano, 2014). In this work, we use the ROMS_AGRIF (Adaptative Grid Refinement in Fortran, https://www.croco-ocean.org/) version developed at IRD/INRIA (Institut de Recherche pour le Développement / Institut National de Recherche en Informatique et en Automatique; Debreu et al., 2012), including algorithms from MARS3D (Model at Regional Scale, http://wwz.ifremer.fr/mars3d) and HYCOM (Hybrid Coordinate Ocean Model, https://hycom.org) ocean models.

Similarly to other studies in the region (*e.g.*, Meccia et al., 2009), ROMS_AGRIF model is applied as a hierarchy of one-way nested, barotropic 2-D models. In this case, the RdP is reached through two domains of different resolution and scale. The lower resolution / largest scale "*Model A*" covers an area spanning from 69 °W to 46 °W and from 59 °S to 26 °S (Fig. 1). Horizontal resolution is set to 7.50´/5.25´ in the zonal/meridional directions, what is equivalent to approximately 12 km. Model A is used to provide boundary conditions to a higher resolution/lower scale model of the RdP (*Model B*, Fig. 1). This model spans the region between 58.75 °W and 52.50 °W, and 38.20 °S and 32.60 °S, with horizontal resolutions of

2.5´/1.75´ in the zonal/meridional directions, respectively (approximately 4 km). This horizontal resolution is consistent with the 1/3 reduction criteria from father to child models.

Tidal forcing is introduced by imposing the elevation at the open boundaries of Model A by means of a bilinear interpolation routine applied to the TPXO8 (http://volkov.oce.orst.edu/tides/tpxo8_atlas.html) 2.00' resolution solution. The eight most important diurnal and semidiurnal tidal constituents are included in the simulations: M_2, S_2, N_2, K_2, K_1, O_1 y P_1.

Given that global bathymetry data bases, like ETOPO, display unrealistic shallow features over Argentinean Continental Shelf, bathymetries for both Model A and B, were built by combining this last data set with data provided by the SHN for depths shallower than 200 m that come from digitalization of nautical charts (SHN, 1986; 1992; 1993; 1999a and b).

3.2. Morris analysis

SA aims to establishing, using different analysis or methodologies:

(i) the relative importance or significance of the different inputs;
(ii) the occurrence of combined effects of a set of inputs on the model solutions;
(iii) and, more broadly, the effect in the output value of changes in a single input, or in a combination of them (Norton, 2015).

The SA presented in this work was made following the methodology suggested by Morris (1991). This methodology is particularly well suited for a model with significant computational overburden as it the case with ROMS_AGRIF. The method ranks the inputs according to their influence on the output and highlights their nonlinearity. In this context, the inputs comprise the equations' coefficients, the model parameters and the properties of the forcings, whereas an output is the value of a variable computed by the model or of any statistic derived from it, such as maximum or mean values.

Morris suggests an efficient algorithm composed of individual randomized one-at-a-time designs, in which the impact of changing the value of each input is evaluated in turn. Campolongo et al. (2007) propose that a large mean of the absolute values of the change due to a particular input indicates a large influence of that input on the model solution. A large standard deviation, in turn, indicates that the effect depends strongly on the input values, implying strong nonlinearity including multilinearity (Morris, 1991).

In this work, the output function chosen to be evaluated in the SA is the root mean square error (RMSE) with respect to the *in situ* observed hourly SSH at Palermo (AMBA, upper estuary; Fig. 1, blue square) and Oyarvide (outer intermediate estuary; Fig. 1, blue circle) tidal stations. The RMSE represents an overall error. In addition to the SA, the comparison of RMSEs for the set of simulations also gives an approach to the set of inputs that yields to a model solution that approximates the observed signal, which is helpful for an eventual fine calibration of the model with a reduced number of simulations. To allow for the inter-comparison among inputs in spite of their order of magnitude, changes were computed using the normalized derivative (Norton, 2015), according to Eq. (1):

$$\frac{\frac{\delta y}{y}}{\frac{\delta p_k}{p_k}} = \frac{p_k}{y}\frac{\delta y}{\delta p_k} \quad (1)$$

where y is the output and p_k is one of the k inputs. The reader is referred to Norton (2015) for further details on the methodology.

3.3. Uncertainties in the meteorological data for ocean model forecast/hindcast at the region of interest

The RdP and the adjacent Continental Shelf are known to be sensitive to atmospheric forcing, in particular to surface winds (Simionato et al. 2004a, b, 2005a, b, 2006a, b, 2007; Meccia et al., 2009). Both direct observations and numerical models have shown that the wind driven circulation at the estuary can be explained in terms of two modes of circulation. The first, prevailing for winds with a cross-estuary component, is related to an inflow/outflow of water at the exterior part of the RdP. The second mode dominates when the wind blows along the estuary axis and has a very distinctive pattern of significant sea level increase or reduction at the upper part of the estuary. In particular, this last mode accounts for the Sudestadas.

Despite its importance, the availability of appropriate atmospheric data to force an ocean forecast model in the region can become a major problem. In fact, the different atmospheric reanalysis database constructed combining numerical models and observations (which are, in theory, much better than forecasts) show important differences when compared to the scarce direct observations over the water in the region. As an example, Fig. 2 shows the wind stress module and direction (reported at a height 10 m) from various data sets for a strong Sudestada event occurred in May, 2000:

a) derived from direct observations collected at Pontón Recalada station (near to Montevideo, Fig. 1) in red; these data have a temporal resolution of 3 hours, i.e. 8-daily.

b) derived from the 4-daily reanalysis from the National Center for Environmental Prediction / National Center for Atmospheric Research – Reanalysis 1 (NCEP/NCAR-RI) (Kalnay et al., 1996) in green;

c) derived from the 4-daily reanalysis from the European Centre for Medium-Range Weather Forecast (ECMWF), ERA-INTERIM, (Dee et al., 2002) in blue;

d) from the 4-daily Blended Sea Winds (BSW) (Zhang et al., 2006) developed by the National Oceanic and Atmospheric Administration (NOAA), in which wind speeds are generated by blending observations from multiple satellites, and the wind directions come from two sources depending on the reanalysis data (NCEP/NCAR-RI) and near-real-time forecast data (ERA-INTERIM), in black.

Table 1 summarizes the main characteristics of every database together with their spatial and temporal resolution.

It is evident from Fig. 2 that all the database reasonably well represent the observed wind direction, but they misrepresent the wind stress module. For the two reanalyses, wind stress displays an important temporal shift on the maximum of the storm (likely to the low temporal resolution), that might eventually produce a temporal error in the simulation of this storm surge if those data were used as forcing. BSW data, presumably because it is based on remote observations and the combination of

reanalyses, provide a better representation of the wind stress module, but does not improve the timing of the storm. Unfortunately, the few available direct observations of wind over the water in the region are not enough to perform a complete assessment of the most convenient data set for the region of interest. Therefore, it is clear that in spite of the database chosen for a simulation, the wind will probably become the main source of errors and uncertainties in the ocean model solutions. Consequently, we decided to incorporate this variable in the SA developed in this paper.

3.4. Analyzed inputs

The inputs chosen for the analysis of this paper correspond to the main forces in the momentum balance of a 2-D barotropic model for a mighty estuary: the energy dissipation by bottom friction, the atmospheric forcing and the continental discharge. More specifically:

a) *Bottom friction*: ROMS_AGRIF considers both a linear and a quadratic coefficient for bottom friction (c_l and c_D, respectively). The bottom friction parameterization considered is Eq. (2):

$$\boldsymbol{\tau}_b = (c_l + c_D w) \cdot \boldsymbol{u} \qquad (2)$$

where $\boldsymbol{\tau}_b$ is the bottom friction stress, w is the module of the velocity, and $\boldsymbol{u}$ is the velocity vector. A mean value of 2.5×10^{-3} for c_D is generally accepted and has been proved to be reasonable for the region (*e.g.*, Simionato et al., 2006a). Here we consider a range of variation between 2.0×10^{-3} and 3.0×10^{-3}. c_l is not a widely-used parameter. ROMS documentation (http://www.myrom.org) suggests that it should be an order of magnitude lower than c_D; thus, to explore its effect on the model solutions we have chosen a broad interval ranging between 1.5×10^{-4} m s^{-1} and 5.0×10^{-4} m s^{-1}.

b) *Wind:* due to the large differences found between the different wind databases for the region (Section 3.3), the evaluation of the impact of the eventual error in the wind forcing is important. We decided to analyze the impact of both the wind speed (w) and direction (Θ) changes. The changes in winds speed are taken into account utilizing a speed factor (I), such that the perturbed speed (w') is w'= Iw. From the observations of Fig. 2, this scalar was chosen to vary between 0.25 and 1.25. In what regards the direction (Θ), its range of variation was estimated using the RMSE of the diverse wind databases of Fig. 2 with respect to the in situ observations at Pontón Recalada station. The obtained value for the analyzed moth was 15°; so, we considered an interval ranging from -15° to 15°. NCEP/NCAR-RI and ERA-INTERIM were chosen as forcings for the simulations. Whereas the first database has a spatial resolution of 0.25° and has been used in other works in the region (*e.g.*, Simionato et al., 2006b; Dragani, et al., 2010), the second one presents a better spacial resolution of 0.125º. This way, the comparison between solutions will provide a first approach to the impact of atmospheric forcing resolution on the simulations.

c) *Continental discharge:* the simulations incorporate the freshwater discharge of the main tributaries to the RdP, the Uruguay River, and the Paraná River on its two main branches (Paraná Guazú-Bravo and Paraná de las Palmas). Observations (Jaime et al., 2002) indicate that runoff can vary in an enormous range, from less than 8,000 m^3 s^{-1} to more than 90,000 m^3 s^{-1}. This input varies in low time frequencies because the runoff of the rivers is regulated by large dams located many kilometers upstream the RdP, and natural variability is mainly dominated by the inter-annual ENSO

cycles. Even though its effect can be in principle regarded as not significant for short time forecast of SSH, it has been recently shown that the tide-current interaction is important in the RdP estuary and that it contributes to the mean sea level (Luz Clara Tejedor et al., 2014). Literature shows, in addition, that for other estuaries the interaction between the surge and the discharge can be large (*e.g.*, Wei-Bo and Wen-Cheng, 2014). It was, therefore, decided to include this input in the analysis for a complete SA. The range of occurrence of the continental discharge was chosen taking into account the observed 10 and 90 percentiles, between 8,000 and 56,000 $m^3 s^{-1}$.

Lateral diffusion (ν) is not considered in the SA because it is known that this parameter does not produce significant changes in 2-D barotropic models (*e.g.*, Simionato et al., 2004b; Bastidas et al., 2016); it was verified for ROMS in a preliminary analysis (not shown) for the region of interest (Dinapoli, 2016). ROMS documentation suggests typical values of this input ranging between 0 and 1,000 $m^2 s^{-1}$. Hence, ν was set at 0 for all the simulations. The chosen ranges of existence for the diverse inputs are summarized in Table 2.

The conversion from wind vectors is made using the quadratic law Eq. (3):

$$\tau_i = c_D^W \rho_A w u_i \quad (3)$$

where *i* represents either the zonal (*x*) or the meridional (y) wind component, $c_D{}^w$ is the wind drag coefficient, ρ_A is the air density, u_i is the wind component and *w* is the wind speed. For the parameterization of the wind drag coefficient we used the expression defined by Bowden (1983), Eq. (4):

$$c_D^w = \begin{cases} 1.1 \times 10^{-3} & , w < 5ms^{-1} \\ \left(1.1 + \frac{2.1}{35} w\right) \times 10^{-3} & , w \geq 5ms^{-1} \end{cases} \quad (4)$$

The wind drag coefficient variation due to changes on wind speed was taken into account in the computation.

4. Results

4.1. Morris analysis

Although different sampling schemes can be used to determinate the trajectories (*e.g.*, Norton, 2015; Campolongo, 2016), in this paper we followed the original Morris design. Overall, 50 trajectories were considered; as 5 parameters were analyzed, 300 simulations were run. As above mentioned, model solutions were compared to SSH observations at Palermo (AMBA, upper estuary) and Oyarvide (outer intermediate estuary) stations (Fig. 1) for a particular Sudestada event occurred on May, 2000, when the maximum height registered at Palermo station was 3.57 m over the Tidal Datum (maximum storm surge). This event was chosen because it is one of the strongest storms ever occurred over the region and it was well studied during the AIACC LA2G Project "Impact of Global Change on the Coastal Areas of the Río de la Plata: Sea Level Rise and Meteorological Effects" (Simionato et al., 2002). The hierarchy of models was run for 61 days, the first 30 corresponding to the spin up of the model, whereas the last 31 were used for the analysis. The time step of the father and child models were, respectively, of 15 and 5 s.

Fig. 3 shows the mean (m) versus the variance (S) of the elementary effects for every input at Palermo (left panel) and Oyarvide (right panel) stations for each wind database, NCEP/NCAR-RI (upper panel) and ERA-INTERIM (lower panel). The red lines indicate the significance. Morris (1991) suggested that the inputs that lay to the right of that line have a mean which is significantly different from zero. The fact that the distribution of the inputs is not same for both wind databases at both stations suggests that inputs are sensitive to local hydrodynamics. However, in every case wind speed was the most important input of the analyzed set, as illustrated by its largest mean. Furthermore, the speed presents a large variance compared to the other inputs, indicating its nonlinear effect on the simulation (Morris, 1991). On the other hand, the fact that the mean of the speed parameter for ERA-INTERIM is greater than for NCEP/NCAR-RI, suggests that ERA-INTERIM has more energy and/or better describes processes at smaller scales, like sea breeze. In fact, it was verified by means of a spectral analyzes (not shown) that peaks at short time scale are more energetic in ERA-INTERIM than in NCEP/NCAR-RI. After the wind, the continental discharge (Q) is the second most important parameter. Its impact decreases towards the outer estuary, consistently with the results of Luz Clara Tejedor (2014) for the interaction between the tide and the continental discharge. Concerning the rest of the inputs, even though they produce changes that are statistically significant, they are very close to the limit of significance. The dissipation parameters, as expected, produce a reduction of the energy of the system, but it is not comparable with the energy apported by the runoff or the wind. Consequently, the selection of those values can be regarded as fine calibration. In spite of the wide range of variability considered (±15°), uncertainties in wind direction do not have a major effect on the simulated signal. This can be attributed to the fact that the chosen variability range (in turn related with the observed differences between wind observations and simulations) maintains the wind direction in the range that produces one of the prevailing modes of circulation of the RdP estuary identified by Simionato et al. (2006a, b).

Summarizing, model solutions are highly (and nonlinearly) sensitive to uncertainties in wind speed, but less sensitive to uncertainties in wind direction. Concerning dissipation by bottom friction, both inputs produce small even significant changes in the simulations. Finally, the runoff has a significant impact in the SSH, but it decreases downstream.

From the 300 different simulations run, it is worthwhile to look for the best combination of inputs that produce the "optimal" solution among this set, to have an idea of the model ability to reproduce the observed surge. The selection of the "optimal" set of parameters was made analyzing the correlation (R) coefficients and the RMSE of the simulated *vs.* the observed storm surge. As the aim of the Project in which this research is framed is to generate storm surge forecasts, the criterion of selection was to choose the set that produces the minimal RMSE and maximal correlation at Palermo station (located at AMBA, in the region of maximum impact of these surges). It should be emphasized that in any case, the selection of this set of parameters in not authentically optimal but a first coarse approximation that must be later refined excluding from the analysis of the relevant parameters and making a fine adjustment of the most important. Fig. 4 shows the storm surge (η_S, left side) obtained by low pass filtering the observed and modelled SSH for periods more than 30 hours at Palermo (upper panel) and Oyarvide (lower panel) stations. Table 3 summarizes the statistical parameters of the simulations and the values of the inputs for each wind database. Here, the slope (P) of the regression line between observations and simulations was added, because it provides an indication of the fit of the simulations to the magnitude of the observations (Meccia et al., 2009). Even though the statistics are satisfactory for both wind databases, a clear improvement is obtained when ERA-INTERIM is used, with a reduction of the RMSE from 0.15 to 0.12 m at Palermo, and 0.21 to 0.13 m at Oyarvide.

Fig. 4 also shows the observed and simulated SSH anomaly obtained by high filtering the simulations for periods less than 30 hs (right side). Variability in this frequency range is mostly due to tides but also includes other short time period

processes (in particular, sea breeze). In both case the model underestimates this signal, but correlation is satisfactory, resulting of 0.84 for Palermo and 0.92 for Oyarvide, for the analyzed month.

4.2. Study of nonlinear interactions between the surge, the tide and the continental discharge

A set of additional processes oriented simulations was performed to study the interactions between the surge, the tide and the continental discharge. For those simulations ERA-INTERIM wind data set was chosen as forcing, due to the best performance shown in the previous section. All the other inputs were kept constant and set at the values of the "optimal" solution. Following Wolf (1978) and Idier (2012), we define the sea level (η) as the addition of the pure effects of the diverse processes considered individually and the interactions among them (η_I). In our case, to the pure tidal level (η_T) and the pure storm surge (η_S) considered by Wolf (1978) and Idier (2012), we add the level produced purely by the runoff (η_R). Therefore, Eq. (5)

$$\eta = \eta_T + \eta_S + \eta_R + \eta_I \quad (5)$$

The results shown in this section correspond to the Sudestada event of May, 2000. To test that the conclusions are independent of the storm surge event considered, the simulations were repeated for another large storm, occurred in August 1991. As this last storm was weaker than that of May 2000 (the maximum peak was of around 2 m over the Tidal Datum), the interactions were also weaker. Nevertheless, both simulations yielded to similar patterns of interaction.

As a reference and to favour discussion, Fig. 5 shows the fields of the maximum absolute value of η (upper left), η_S (upper right), η_T (lower left) and η_R (lower right). The pure surge (η_S) shows the characteristic pattern of the normal mode of the RdP excited by winds from the southeast sector (Simionato et al., 2004a): isolines are perpendicular to the estuary axis, and elevations increase towards the estuary head. Maximum values for this storm are over 4.25 m, showing the strength of this event. The pure tide (η_T) illustrates how the tidal wave progresses along the estuary coasts as a Kelvin wave forced at the mouth (Simionato et al., 2004b). Maximum amplitudes occur at Samborombón Bay, reaching 1 m, and decay towards the estuary head due to the loss of energy by bottom friction (Simionato et al., 2004b). As the wave propagates over shallower regions (Fig. 1), the wavelength decreases, so that one complete wave can be seen at the estuary all the time (Framiñan et al., 1999). Finally, the SSH anomaly due to the river discharge (η_R) shows how the plume is deviated to the left (in the Southern Hemisphere) by the Coriolis force (Simionato et al., 2004a). It must be taken into account that even though the RdP is small, it is also very shallow, and the (barotropic) Rossby radius of deformation ($R = \sqrt{gH}/f$, where g is the acceleration due to gravity, H is the depth and f is the Coriolis parameter) is around only 100 km. The elevations associated to the runoff are of a few centimetres but it affects mean currents.

The upper left panel of Fig. 6 shows the maximum value of the magnitude of η_I (absolute value) at every model grid point. Interactions are larger along the southern coast of the RdP, consistently with the direction of propagation of the tide (lower left panel of Fig. 5). Two well differenced zones of maximum η_I are found. The first is located along Samborombón Bay coasts, extending to the north of Punta Piedras; these are the areas where the tide is largest and the energy dissipation by bottom friction maximizes at the RdP (Simionato et al., 2004b). The absolute maximum occurs at the upper estuary, close to the mouths of the main tributaries to the estuary, *i.e.*, this is the region where the interaction with the continental discharge is

expected to maximize (see lower right panel of Fig. 5). Interactions have large values, of up to 0.45 m, what is significant compared to the magnitude of the tides in the area the RdP has a microtidal regime with amplitudes in the order of 0.5 m at the upper estuary (Simionato et. al, 2004b).

For a better understanding of the interactions, new simulations were run to analyze them by pairs. Following the formulation proposed by Wolf (1978) we defined:

a) $\eta^{I}_{TR} = \eta_{TR} - (\eta_T + \eta_R)$, the tide-runoff interaction;

b) $\eta^{I}_{TS} = \eta_{TS} - (\eta_T + \eta_S)$, the tide-surge interaction;

c) $\eta^{I}_{SR} = \eta_{SR} - (\eta_S + \eta_R)$, the surge-runoff interaction.

Here, the superscript *I* denotes "interaction" and the subscripts indicate the processes considered in the simulations: *T* for tide, *S* for surge and *R* for runoff. Fig. 6 shows the three fields of maximum absolute value of the interaction for η^{I}_{TS} (upper right), η^{I}_{TR} (lower left) and η^{I}_{SR} (lower right); note that the scales of the figures are different. Comparing these interactions with η_I (upper left panel of Fig. 5), it emerges that the principal nonlinear interaction in the RdP is between the tide and the surge (η^{I}_{TS}, upper right), with the largest values of interaction of around 0.35 m. Tide-surge interaction has two regions of maxima: one at Samborombón Bay, where the tidal amplitude and dissipation by bottom frictions are largest in the RdP (Simionato et al., 2004b), and another at the very shallow (around 2 m) upper estuary (Fig. 1). The interaction is much lower along the Uruguayan coast, where tides there are weak (Fig. 5 lower left panel). The order of magnitude of the interaction (0.35 m) indicates that the omission of tides in a storm surge model of the upper and intermediate estuary would drive to an error of around 10%. The surge-runoff interaction (η^{I}_{SR}, lower right panel of Fig. 6) is the smallest of the three studied, maximizing at the upper estuary with a value of around 0.08 m and decaying offshore as the impact of the river discharge decays (see lower left panel of Fig. 5). Finally, tide-runoff interaction (η^{I}_{TR}, lower left panel of Fig. 6) is lower than η^{I}_{TS} but larger than η^{I}_{SR} and has an impact only at the upper and intermediate estuary. In this sense, even though the plume reaches the exterior RdP (lower right panel of Fig. 5), the tides along the northern coast of the estuary are very weak (lower left panel of Fig. 5).

Finally, Fig. 7 shows time series of the evolution of the SSH at three selected points where maximum values of interaction (upper left panel of Fig. 6) were observed: Guazú (left), Palermo (centre) and Samborombón (right). These locations are shown as a circle, a triangle and a square, respectively, in Fig. 6). The series were extracted from models with of pure tide ("tide", red), pure surge ("surge", green), pure continental discharge ("river", yellow), and tide, surge and runoff together ("sea level", blue). Additionally, the "practical" surge (magenta) is calculated as the addition of the pure tide, pure surge and pure runoff SSH anomalies. Finally, the "interaction" signal (black) is computed as the difference between the full model and the practical surge, representing the nonlinear residual effects (Eq. 3). In every case this interaction becomes stronger during the storm surge event and is opposite to the practical signal, indicating that the interaction brings energy from low frequencies to high frequencies.

4.3. Quantification of the influence of the continental discharge

In the previous section we showed that the continental discharge significantly interacts with the surge and the tide. Nevertheless, from the practical point of view of an SSH forecast model, it is important to know the sensitivity of the solutions to potential errors in the "predicted runoff" included in the simulations. Due to the fact that the processes that control the discharge to the RdP are of large scale, they vary essentially in inter-annual time scales and are virtually independent of the processes that produce the storms. Therefore, in this estuary the coupling of a hydrological forecast model would be unnecessary for SSH operational forecast purposes unless the above mentioned sensitivity is high. For this reason a last set of simulations was performed in which all the inputs with exception of the continental discharge were kept constant and set at the values of the "optimal" solution. Runoff was varied from 0 to 56,000 $m^3 s^{-1}$, at steps of 8,000 $m^3 s^{-1}$. Although the last value is not the maximum registered, it is representative of the percentile 90 of the historical continental discharge.

Fig. 8 shows a comparison of the evolution of the SSH anomaly between the extreme simulations with a continental discharge of 56,000 $m^3 s^{-1}$ (yellow) and without runoff (magenta), for Guazú (left), Palermo (centre) and Samborombón (right). It is evident from the figure that the main effect of the discharge is to produce a change in the mean sea level or "shift" among solutions. Nevertheless, even smaller in magnitude, the continental discharge and the interactions also produce a deformation of the tidal wave and the storm surge. This is a result of the interaction with the current due to the runoff: when the tidal wave or storm surge propagates upstream (downstream), the associated currents are in the opposite (same) direction than the river flow and therefore the wave becomes "steeper" ("gentler"). Both effects decay with the distance to the sources, being almost negligible at Samborombón.

To quantify the above mentioned effects for the different discharges above mentioned, Fig. 9 shows the root mean square difference between the sea level anomaly computed for models with and without runoff, as a function of the runoff, for Guazú (left), Palermo (center) and Samborombón (right) stations (see locations in Fig. 6). The differences were computed for the "full" sea surface height anomaly (green line), the high pass filtered height with a cut-off period of 30 hours ("tide", red) and the low pass filtered height with the same cut-off period ("surge", blue). Note that the addition of the "surge" and the "tide" lines is considerably smaller than the "full" signal, because this last includes the setup due to the runoff, which in all the cases is larger than the nonlinear effects of interaction with the tide and the surge. Consistently with previous results, the general impact of the runoff decreases towards the outer estuary, being 50 times smaller at Samborombón than at Guazú. Finally, it can be observed that both the setup and the nonlinear interactions grow almost linearly with the discharge. Even though there is sensitivity with the discharge, the figure suggests that the impact of a small error in the runoff on the forecast of the surge is small, and that, therefore, the coupling of a hydrological model to the hydrodynamic one is unnecessary for short range forecast.

5. Summary of conclusions and final remarks

In this work, we discussed a sensitivity analysis (SA) based on Morris methodology, which is particularly well suited for models with large computational demand, to determine the sensitivity of numerical solutions for the Southwestern Atlantic Continental Shelf with emphasis in the wide and fast flowing RdP estuary to different parameters. An evaluation of the overall model SA the most critical storm event for the inhabitants of the region and for navigation, known as Sudestada, was

permormed. The results from the SA reduce the required number of simulations needed for model calibration, reducing the future work to the fine calibration of the most sensitive inputs.

ROMS_AGRIF model was chosen to build the pre-operational forecast model. It was applied in a hierarchy of 2-D one-way nested grids with refinement of the solutions over the RdP estuary.

The SA was made including the bottom friction quadratic (c_D) and linear (c_l) parameterizations. Due to the scarcity of direct wind observations over the estuary and the limitations in the numerical modelling of the winds in the area, wind data becomes a significant source of errors and uncertainties for any ocean forecast model. Hence, wind speed (through a factor I) and direction (Θ) were included in the SA. Finally, the RdP is very mighty, and continental discharge can vary significantly (in a range of around 80,000 $m^3 s^{-1}$) in the period of a few months, becoming also an important input which influence must be assessed. The ranges of existence of every input were set using values from literature, the RMSE with respect to observations, and extremes observed values, respectively.

The sensitive analysis showed significant model response to all the considered inputs. The most important, with nonlinearity in the model response, was the wind speed (I). In particular, the model response showed to be very sensitive even to small changes in this forcing. The next most important input is Q, which response is more linear and presents a regional dependence, becoming less important towards the outer estuary (*i.e.*, downstream). Finally, model solutions are relatively much less sensitive to Θ, c_D and c_l.

With the objective of further helping on the decision of how to built a numerical forecast strategy for SSH anomaly in the RdP, we also analyzed the interactions between the surge, the tide and the runoff. Results indicate that the interactions are important, accounting for around 10% of the total SSH anomaly during the storm. The most significant interaction (approximately 90% of the total) occurs between the surge and the tide, maximizing at Samborombón Bay and the upper RdP. The interaction between the tide and the runoff is much weaker, of the order of 10% of the amplitude of the tide. Finally, the interaction between of the runoff and the surge is of similar order of magnitude than that of the tide with the runoff. The last two interactions maximize at the upper estuary (where the tributaries flow to the RdP) and decay offshore, being almost negligible at the outer RdP.

The results of this research provide information that will allow an optimal calibration of the model with only a fine tuning and a minimum number of simulations in the next future. They also highlight some the needs to face the construction of an accurate numerical forecast system for the prediction of extreme surges in the RdP. In this sense, we can conclude that:

a) The fact that the model solutions are extremely sensitive to small uncertainties in the wind speed indicates that the most obvious way of improving the surge forecast is either improving the atmospheric forcing or at least quantifying the forecast error due to the uncertainties. Some ways of improving the wind forcing is by increasing the temporal and spatial resolution, and the diversity of physical processes included in the simulations, by the use of regional numerical models and/or assimilating data on the simulations. For this, more direct observations over the RdP would be necessary. As an intermediate step, an empirical adjustment of the winds could be attempted. The uncertainties in the SSH anomaly forecast can be quantified by ensemble modelling.

b) The inclusion of the continental discharge in a forecast model for the SSH anomaly in the RdP is fundamental. Its main effect is to introduce a setup (or SSH elevation), but also interacts with the tide and the surge, particularly in the upper estuary, where the most populated areas of the RdP coasts are located and where, in consequence, the impact of the floods maximizes. Nevertheless, the fact that the variability of the runoff is uncoupled with the surge, warranties that small uncertainties in the value of the discharge will not introduce large errors in the surge forecast. In this sense, for short term forecast the coupling of a hydrological model to the hydrodynamic one is unnecessary.

c) Finally, it is absolutely necessary to include tides in the simulation. The tide has strong interactions with the surge, accounting for approximately 10% of the total signal. Furthermore, the tide interacts with the runoff, introducing more modifications in the real surge.

6. Acknowledgements

This study was funded by the National Agency for Scientific and Technological Research of Argentina (ANPCyT) PICT 2014-2672 Project, the Programa de Investigación y Desarrollo para la Defensa del MINDEF (PIDDEF) 14-14 Project, and the UBACYT 20020150100118BA directed by Claudia G. Simionato. Matías G. Dinapoli participation was possible thanks an ANPCyT PhD fellowship.

References

Acha, E.M., and Macchi, G.J.: Spawning of Brazilian menhaden, Brevoortia aurea, in the Río de la Plata estuary off Argentina and Uruguay, Fishery Bulletin, 98, 227-235, 2000.

Balay, M. A.: El Río de la Plata entre la Atmósfera y el Mar. Publicación H-621. Servicio de Hidrografía Naval, Armada Argentina, Buenos Aires, 153 pp, 1961.

Bastidas, L. A., Knighton, J., and Kline, S. W.: Parameter sensitivity and uncertainty analysis for a storm surge and wave model, Nat. Hazards. Earth. Syst. Sci., 16:2195-2210, doi:10.5194/nhess-16-2195-2016, 2016.

Boschi, E.E.: El ecosistema estuarial del Río de la Plata (Argentina y Uruguay). Anales del Instituto de Ciencias del Mar y Limnología, Universidad Nacional Autónoma de México, 15, 159-182., 1988.

Bowden, K.F., 1983. Physical Oceanography of Coastal Waters. In: Caldwell, D.K., Anderson, W.W. Eds.). Ellis Horwood Ltd, Chichester, UK, 302 pp.

Campolongo, F., Cariboni, J., and Saltelli, A.: An effective screening design for sensitivity analysis of large models, Environ. Modell. Softw., 22:1509–1518, 2016.

Campos, J. D., Lentini, C. A., Miller, J. L., and Piola, A. R.: Interannual variability of the sea surface temperature in the South Brazilian Bight, Geophys. Res. Lett., 26(14), 2061-2064, 1999.

Combes, V., and Matano, R. P.: A two-way nested simulation of the oceanic circulation in the southwestern atlantic, J. Geophys. Res.: Ocean, 119(2):731-756, 2014.

D'Onofrio, E. E., Fiore, M. E., and Romero, S.: Return periods of extreme water levels estimated for some vulnerable areas of Buenos Aires, Cont. Shelf Res., 19:1681-1693, 1999.

Debreu, L., Marchesiello, P., Penven, P., and Cambon G.: Two-way nesting in split-explicit ocean models: algorithms, implementation and validation, Ocean. Model., 49-50, 1-21, 2012.

Dee, D. P., Uppala, S. M., Simmons, A. J., Berrisford, P., et al.: The ERA-Interim reanalysis: configuration, performance of the data assimilation system, Q. J. Roy. Meteorol. Soc., 137, (656) 553-597, doi: 10.1002/qj.828, 2011.

Dinapoli, M. G.: Estudio de la sensibilidad de un modelo barotrópico 2-D para la predicción del nivel del mar. Dissertation, Facultad de Ciencias Exactas y Naturales, Universidad de Buenos Aires, 2016.

Dragani, W. C., Martín, P., Campos, M. I., and Simionato, C.: Are wind wave heights increasing in southeastern south American continental shelf between 32S and 40S?, Cont. Shelf Res., 30, (5) 481-490, doi:10.1016/j.csr.2010.01.002, 2010.

Escobar, G., Vargas, W., and Bischoff, S.: Winds tides in the Río de la Plata estuary: meteorological conditions, Int. J. Climatol., 24, 1159-1169, 2004.

Framiñan, M. B., Etala, M. P., Acha, E. M., Guerrero, R. A., Lasta, C. A., and Brown, O. B.: Physical characteristics and processes of the Río de la Plata Estuary, in Estuaries of South America: Their morphology and dynamics, edited by Perillo, G.M.E, Piccolo, M.C., and Pino Quivira, M., Springer, Berlín, pp. 161-194, 1999.

Flather, R. A.: Storm surge, in: Encyclopedia of Ocean Sciences, edited by: Steele, J. H., Thorpe, S. A. and Turekian, K. K., Academic, San Diego, Calif, 2882-2892, 2001.

Gan, M. A., and Rao, V.B.: Surface cyclogenesis over South America. Monthly Weather Review 119(5), 1293–1302, 1991.

Guerrero, R. A., Piola, A. R., Molinari, G. N., Osiroff, A. P., and Jáuregui, S. I.: Temperature and salinity climatology in the Río de la Plata and its Maritime Front. Argentina-Uruguay, Mar del Plata: Instituto Nacional de Investigación y Desarrollo Pesquero INIDEP, 95 pp, 2010.

Klerk, W. J., Winsemius,H. C., van Verseveld, W. J., Bakker, A. M. R., and Diermanse, F. L. M.: The co-incidence of storm surges and extreme discharges within the Rhine–Meuse Delta, Environ. Res. Lett., Vol. 10, 3, 2015.

Idier, D., Dumas, F., and Muller, H.: Tide-surge interaction in the English Channel, Nat. Hazards Earth Syst. Sci., 12, 3709-3718, doi: 10.5194/nhees-12-3709-20102, 2012.

Jaime, P., Menéndez, A., Uriburu Quirno, M., and Torchio, J.: Análisis del régimen hidrológico de los ríos Paraná y Uruguay, Informe LHA 05-216-02, Instituto Nacional del Agua, Buenos Aires, Argentina, 2002.

Jaureguizar, A., Bava, J., Carozza, C., and Lasta, C.: Distribution of the whitemouth croaker (micropogonias furnieri) in relation to environmental factors at the Rio de la Plata estuary, South America, Mar. Ecol. Prog. Ser., 255, 271-282, 2003b.

Jaureguizar, A., Militelli, M., and Guerrero, R.: Distribution of micopogonias furnieri at different maturity stages along an estuarine gradient and in relation to environmental factors, J. Mar. Biol. Assoc. U. K., 88(1):175-181, 2008.

John Maskell, Kevin Horsburgh, Matthew Lewis, and Paul Bates.: Investigating River–Surge Interaction in Idealised Estuaries. Journal of Coastal Research: Volume 30, Issue 2: pp. 248 – 259.

Kalnay et al.,The NCEP/NCAR 40-year reanalysis project, Bull. Amer. Meteor. Soc., 77, 437-470, 1996.

Luz Clara Tejedor, M. : Cambios en la propagación de la onda de marea en la Plataforma Continental y el Río de la Plata, asociados a cambios en el nivel medio del mar y los ciclos de la descarga continental. PhD Dissertation, Facultad de Ciencias Exactas y Naturales, Universidad de Buenos Aires, 2014.

Luz Clara Tejedor, M., Simionato, C. G., D'Onofrio, E. E., Fiore, M. M. E., and Moreira, D.: Variability of tidal constants in the Río de la Plata estuary associated to the natural cycles of the runoff, Estuar. Coastal Shelf S., (7) 148:85-96, 2014.

Maskell, J., Horsburgh, K., Lewis, M., and Bates, P.: Investigating River–Surge Interaction in Idealised Estuaries, J. Coastal Res., Volume 30, Issue 2: pp. 248 – 259, 2014.

Meccia, V.L., Simionato, C.G., Fiore, M.M.E., D'Onofrio, E., and Dragani, W.: Sea surface height variability in the Río de la Plata estuary from synoptic to inter-annual scales: results of numerical simulations, Estuar. Coast. Shelf Sci., 85(2), 327-343, doi:10.1016/j.ecss.2009.08.024, 2009.

Morris, M. D.: Factorial sampling plans for preliminary computational experiments, Technometrics, 33:161–174, 1991.

Nagy, G. J., Martinez, C. M., Caffera, R. M., Pedraloza, G., Forbes, E. A., Perdomo, A. C., and Laborde, J. L.: The hydrological and climatic setting of the Río de la Plata. In: The Río de la Plata. An Environmental Review, An Eco Plata Project Background Report, Dalhausie University, Halifax, Nova Scotia, pp. 17—68, 1997.

Necco, G.: Comportamiento de vórtices ciclónicos en el área sudamericana durante FGGE: Ciclogénesis. Meteorológica, 13, 7–20, 1982.

Norton, J. P.: An introduction to sensitivity assessment of simulation models, Environ. Modell. Softw., 69:166—174, 2015.

Piola, A. R., Campos, E. J., Möller, O. O., Charo, M., and Martinez, C.: Subtropical Shelf Front off eastern South America, J. Geophys. Res., 105(C3), 6565-6578, 2000.

Robertson, A., and Mechoso, C. R.: Inter-annual and decadal cycles in river flows of southeastern South America, J. Climate, 11:2570-2581, 1998.

Rossiter, J. R.: Interaction between tide and surge in the Thames, Geophys. J. R. Astron. Soc., 6, 29-53, 1961.

Satelli, A., Chan, K., and Scott, E. M..: Sensitivity Analysis, Wiley, Chischester, UK, 2000.

Seluchi, M. E.: Diagnóstico y pronóstico de situaciones sinópticas conducentes a ciclogénesis sobre el este de Sudamérica, Geofis. Int., 34:171-186, 1995.

Seluchi, M. E., and Saulo, A. C.: Possible mechanisms yielding an explosive cyclogenesis over South America: Experiments using a limited area model, Aust. Meteorl. Mag., 47:309-320, 1996.

Shchepetkin, A. F., and McWilliams, J. C.: The Regional Ocean Modeling System: A split-explicit, free-surface, topography following coordinates ocean model, Ocean Model., 9:347-404, 2005.

Shiklomanov, I. A.: A Summary of Monograph World Water Resources: A New Appraisal and Assessment for the 21st Century, Report U. N. Environ. Programme., Nairobi, 1998.

SHN, Mar Argentino, de Río de la Plata al Cabo de Hornos, Carta Náutica 50, 4th edition, Servicio de Hidrografía Naval, Armada Argentina, 1986.

SHN, Acceso al Río de la Plata, Carta Náutica H1, 5th edition, Servicio de Hidrografía Naval, Armada Argentina, 1992.

SHN, El Rincón, Golfo San Matías y Nuevo, Carta Náutica H2, 4th edition, Servicio de Hidrografía Naval, Armada Argentina, 1993.

SHN, Río de la Plata Medio y Superior, Carta Náutica H116, 4th edition, Servicio de Hidrografía Naval, Armada Argentina, 1999a.

SHN, Río de la Plata Exterior, Carta Náutica H113, 2nd edition, Servicio de Hidrografía Naval, Armada Argentina, 1999b.

Simionato, C. G., Nuñez, M., and Meccia, V.: Estudio de la respuesta del modelo HamSOM/CIMA a vientos intensos sobre el Río de la Plata, CIMA/CONICET-UBA, Inform CIMA / Oc-02-01. 61 pp, 2002.

Simionato, C. G., Dragani, W. C., Meccia, V. L., and Nuñez, M. N.: A numerical study of the barotropic circulation of the Río de la Plata Estuary: sensitivity to bathymetry, the earth's rotation and low frequency wind variability, Estuar. Coast. Shelf Sci., 61:261-273, 2004a.

Simionato, C. G., Dragani, W. C., Nuñez, M. N., and Engel, M.: A set of 3-D nested models for tidal propagation from the Argentinian Continental Shelf to the Río de la Plata Estuary: I. M_2, J. Coastal Res., (3) 20:893-912, 2004b.

Simionato, C. G., Meccia, V. L., Dragani, W. C., and Nuñez, M. N.: Barotropic tide and baroclinic waves observations in the Río de la Plata Estuary, J. Geophys. Res., 110, C06008, doi: 10.1029/2004JC002842, 2005a.

Simionato, C. G., Vera, C., and Siegismund, F.: Surface wind variability on seasonal and inter-annual sacales over Río de la Plata area, J. Coastal. Res., (4) 21:770-783, 2005b.

Simionato, C. G., Meccia, V. L., Dregani, W. C., Guerrero, R. A., and Nuñez, M. N.: The Río de la Plata Estuary response to wind variability in synoptic to intra-seasonal scales: Barotropic response, J. Geophys. Research, 111, C09031, doi: 10.1029/2005JC003297, 2006a.

Simionato, C. G., Meccia, V. L., Dragani, W. C., and Nuñez, M. N.: On the use of the NCEP/NCAR surface winds for modelling barotropic circulation in the Río de la Plata Estuary, Estuar. Coast. Shelf. S., 70:195-206, 2006b.

Simionato, C. G., Meccia, V. L., Guerrero, R. A., Dragani, W. C., and Nuñez, M. N.: Río de la Plata Estuary response to wind variability in synoptic to inter-seasonal scales: 2. Current's vertical structure and its implications for the salt wedge structure, J. Geophys. Res., 112, C07005, doi: 10.1029/2006JC003815, 2007.

Sinclair, M.R.: An objective cyclone climatology for the southern hemisphere. Monthly Weather Review, 122, 2239–2256, 1994.

Strub, P. T., et al.: Altimeter-derived seasonal circulation on the southwest atlantic shelf: 27°-43°S, J. Geophys. Res. Oceans, 120(5), 3391-3418, doi:10.1002/2015JC010769, 2015.

Tonini, M. H., and Palma, E. D.: Circulación residual y vorticidad mareal en los golfos norpatagónicos. Asociación de Mecánica Computacional XXVIII, 2851-2867, 2009.

Vera, C., Vigliarolo, P. K., and Berbery, E. H.: Cold season synoptic scale waves over subtropical South America, Mon. Wheather Rev., 130:684—699, 2002.

Wie-Bo C., and Wen-Cheng, L.: Modeling Flood Inundation Induced by River Flow and Storm Surges over a River Basin, Water , 6, 3182-3199; doi:10.3390/w6103182, 2014.

Wolf, J.: Interaction of tide and surge in a semi-infinite uniform channel, with application to surge propagation down the east coast of Britain, Appl. Math. Modelling, 2, 245-253, 1978.

Zhang, H-M., Bates, J. J., and Reynolds, R. W.: Assessment of composite global sampling: Sea surface wind speed, Geophys. Res. Lett., 33, L17714, doi: 10.1029/2006GL027086, 2006.

Figures

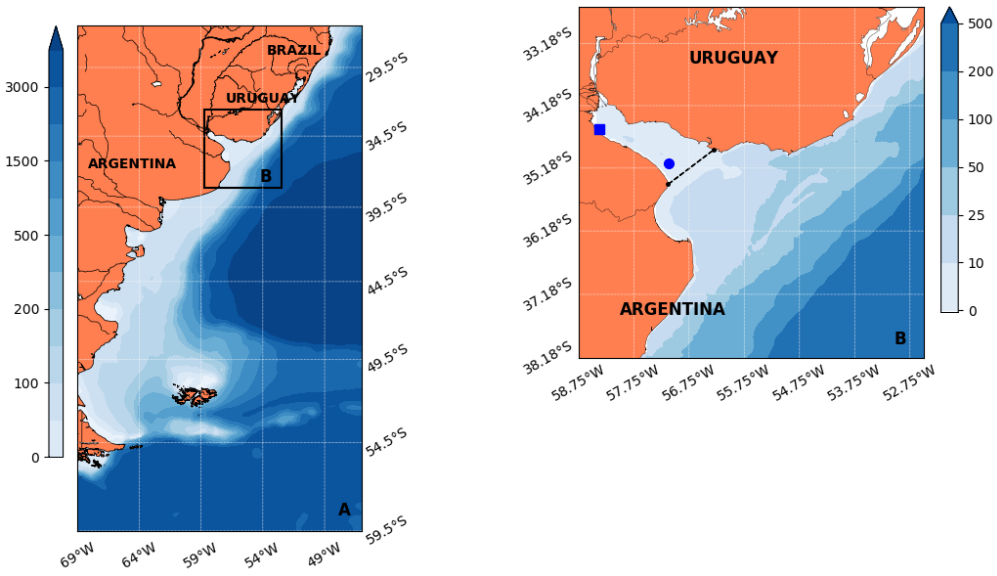

Figure 1. Map of the study area, showing the domain of the two nested models (A and B). The isolines represent the bathymetry (in m).The location of the tide gauges, Palermo (or AMBA) and Oyarvide, are shown as a blue square and a blue circle, respectively. The black dashed line shows the location of the Barra del Indio shoal. It goes from Punta Piedras in Argentina to Montevideo in Uruguay.

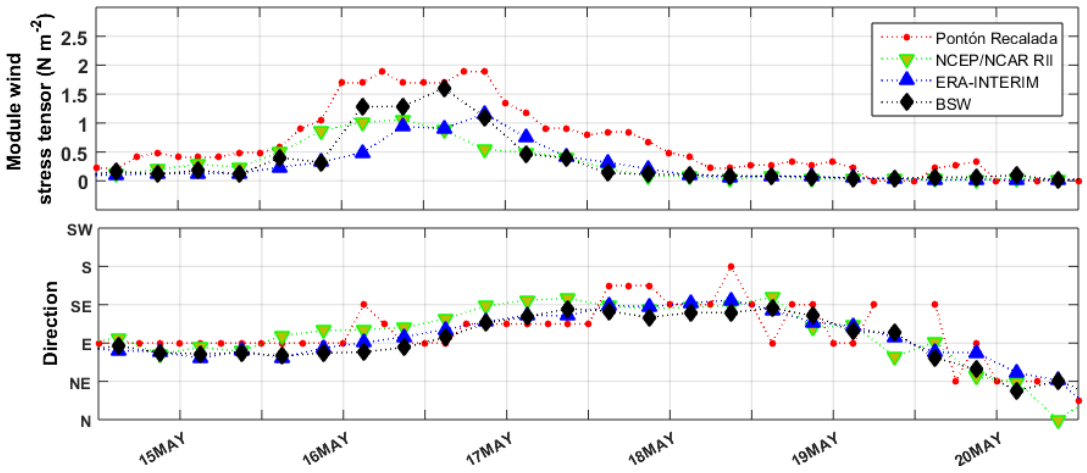

Figure 2. Wind stress module (upper panel) and direction (lower panel) from different global analysis *vs*. observations at Pontón Recalada station during the Sudestada event occurred on May, 2000. The figure corresponds to the period 5/15/2000 12:00 GMT – 5/20/2000 12:00 GMT.

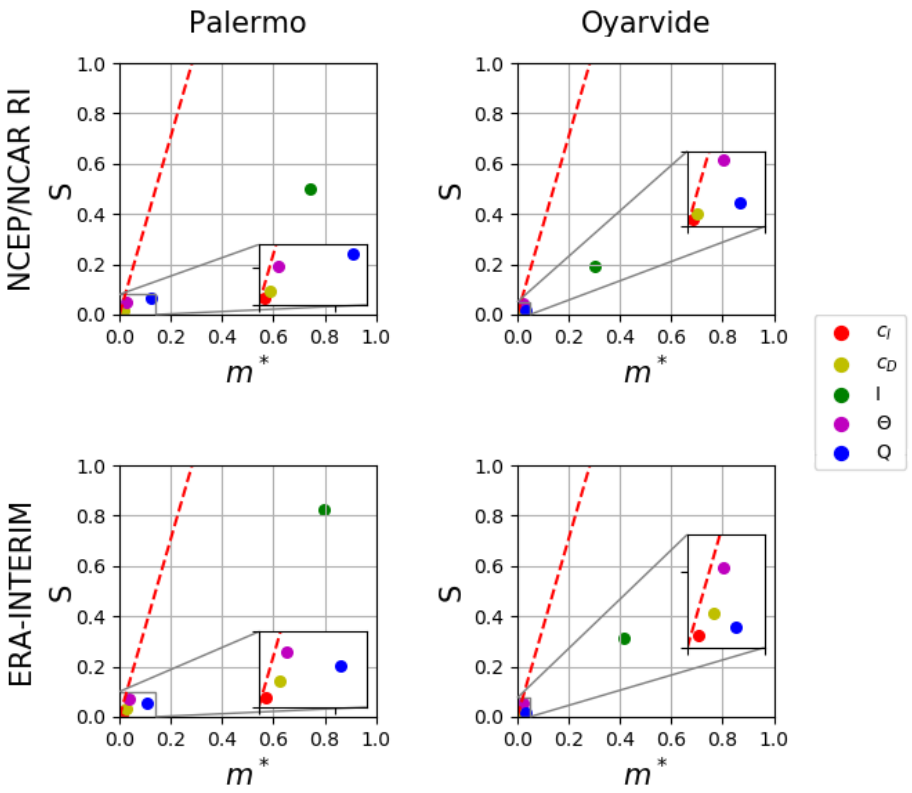

Figure 3. Estimated means (m*) and standard deviation (S) for SSH at Palermo (left side) and Oyarvide (right side) stations for NCEP/NCAR-RI (upper panel) and ERA-INTERIM (lower panel) atmospheric forcing. The red line corresponds to m = 2×SEM, standard error of the mean.

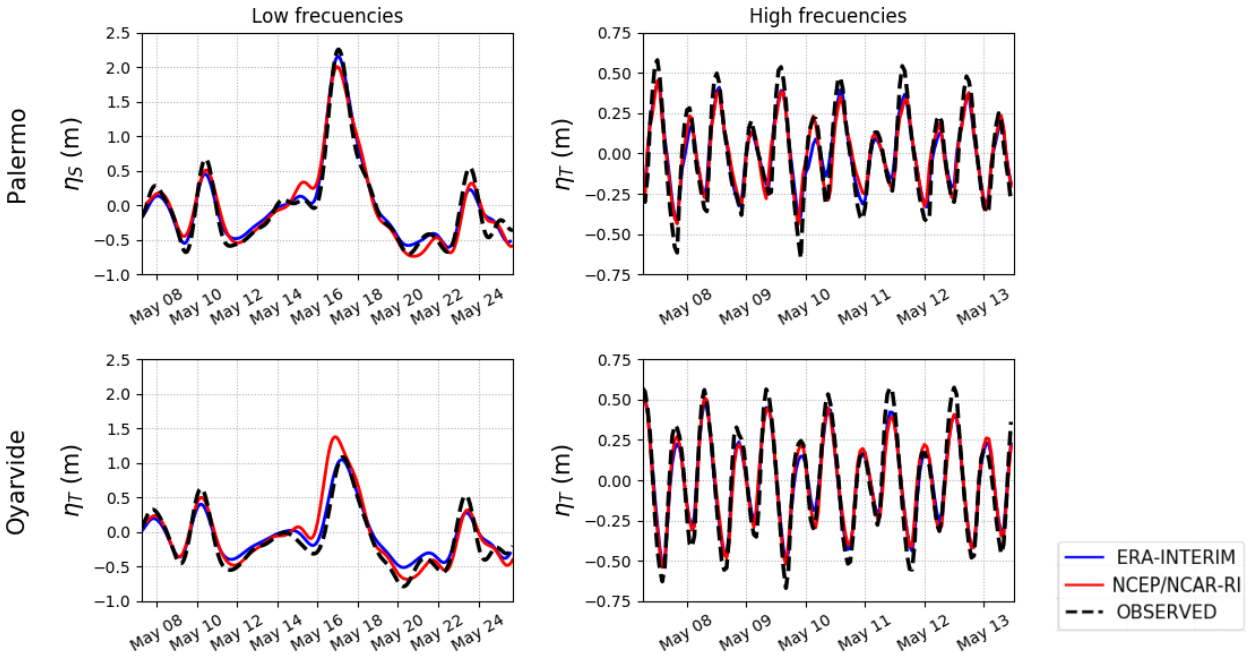

Figure 4. Low pass (η_S, left side) and high pass (η_T, right side) filtered SSH computed from simulation forced with ERA-INTERIM (blue full line) and NCEP/NCAR-RI (red full line) winds, for the set of inputs that minimize the RMSE with respect to the observed η_S (black dashed line), at Palermo (upper panel) and Oyarvide (lower panel) stations during the Sudestada event of May 2000.

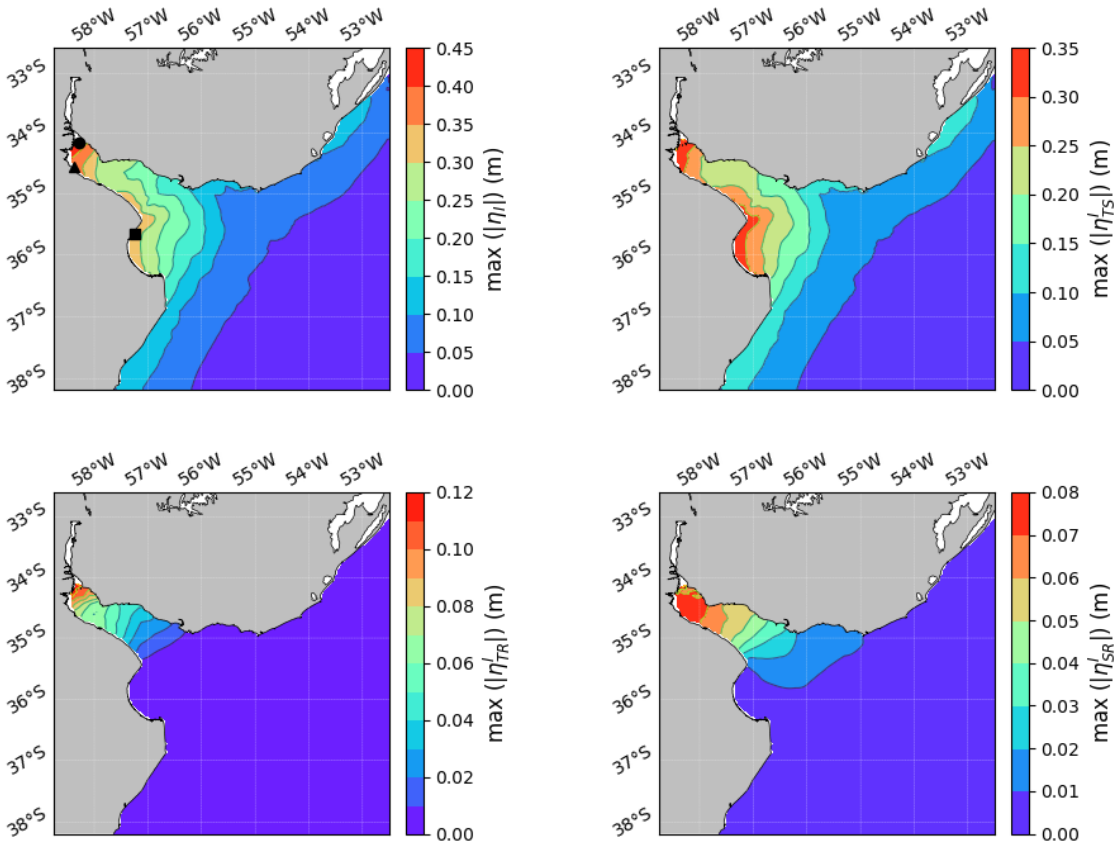

Figure 5. Maximum absolute value of the SSH anomaly for a "full" model (η, upper left), a pure storm surge model (η_S, upper right), a pure tide model (η_T, lower left) and a pure continental discharge model (η_R, lower right) during the Sudestada event of May, 2000. Note that every subplot has different colour scale.

Figure 6. Maximum absolute value of the tide-surge-runoff interactions in a "full" model (η_I, upper left), the surge-tide interaction in a "tide-surge" model (η^I_{TS}, upper right), the tide-runoff interaction in a "tide-runoff" model (η^I_{TR}, lower left) and surge-runoff interaction in a "surge-runoff" (η^I_{SR}, lower right) during the Sudestada event of May, 2000. Note that every

plot has different colour scale. The black circle, triangle and square in the upper left plot show the location of Paraná-Guazú, Palermo and Samboronbón.

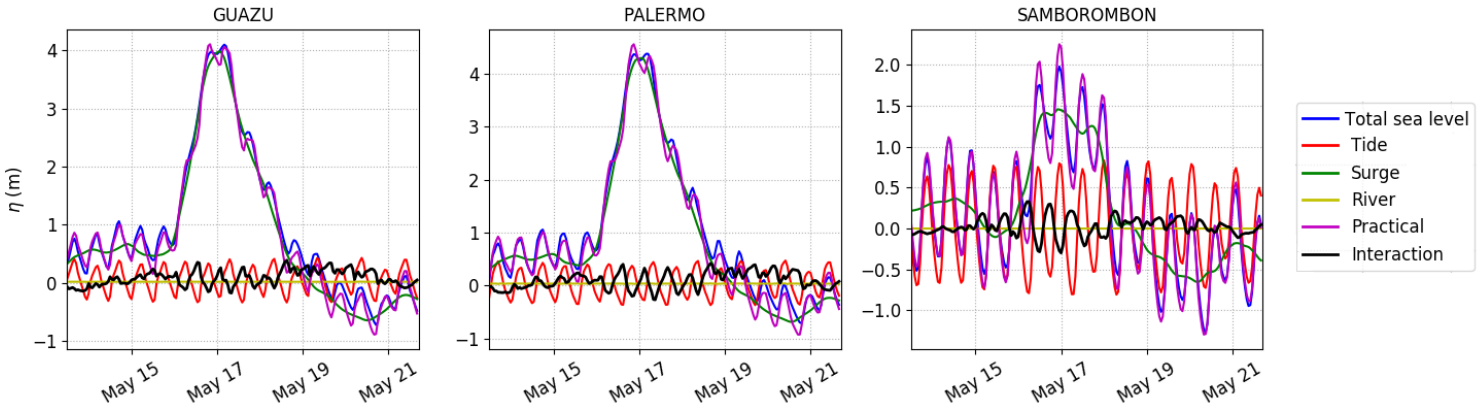

Figure 7. Time series at Guazú (left), Palermo (centre) and Samborombón (right) during the storm surge of May, 2000 from a "full" model (blue), a "pure tide" model (red), a "pure storm surge" model (green) and a "pure continental discharge" model (yellow). The practical surge is displayed in magenta and the residual interaction in black. Note that every subplot has a different vertical scale.

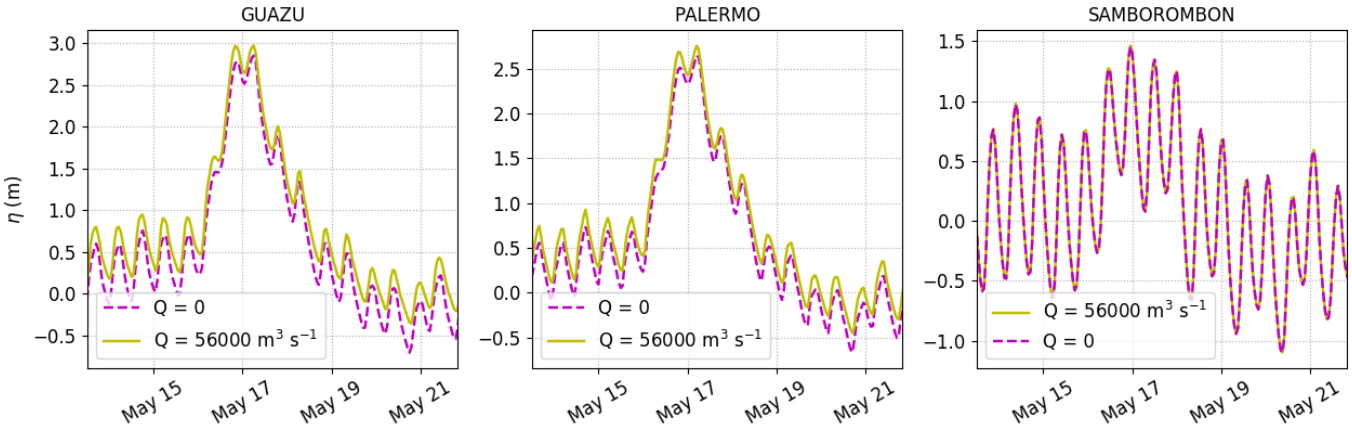

Figure 8. Time series of the total sea elevation (η) during the Sudestada event of May, 2000 at Guazú (left), Palermo (centre) and Samborombón (right), for simulations without runoff (magenta dashed line) and with a runoff of the 56,000 m^3 s^{-1} (yellow solid line). Note that every subplot has a different vertical scale.

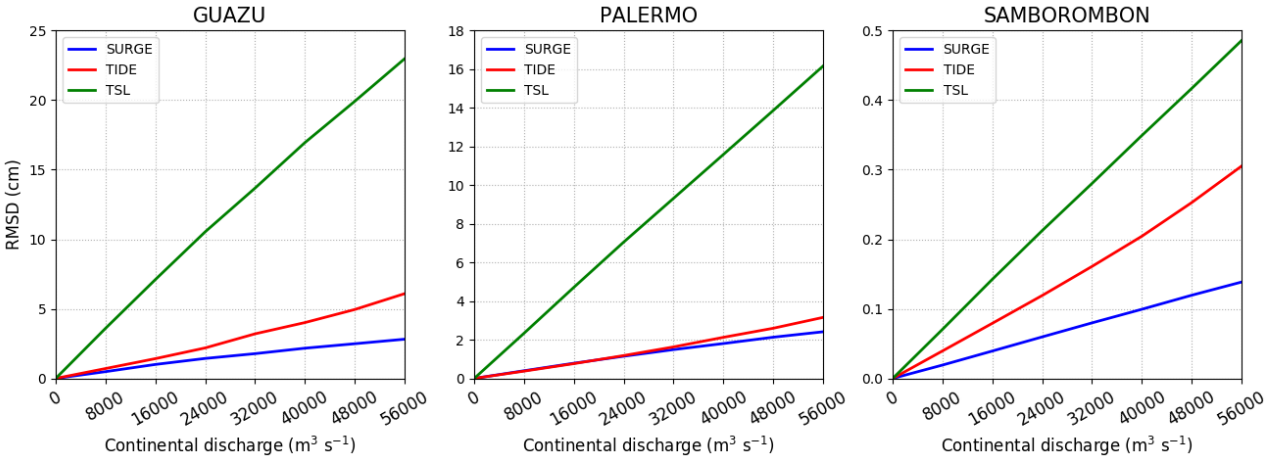

Figure 9. Root mean square difference (RMSD) of the total sea level (TSL, green), tide (TIDE, red) and storm surge (SURGE, blue) for models with diverse continental discharges with respect to one without continental discharge, as a function of the discharge, at Guazú (left), Palermo (centre) and Samborombón (right) during Sudestada event of May, 2000. Note that every subplot has a different vertical scale.

Tables

Table 1. Summary of the spatial and temporal resolutions of the different wind data sets utilized in the construction of Fig. 2.

Base data	**Type**	**Spatial resolution**	**Temporal resolution**
Pontón Recalada	Direct observation	-	3 hours
NCEP/NCAR RI	Re-Analysis	0.25° (28 km)	6 hours
ERA-INTERIM	Re-Analysis	0.125° (14 km)	6 hours
BSW	Blended	0.25° (28 km)	6 hours

Table 2. Inputs considered for the SA and their ranges of existence.

Input	**Interval**	**Unit**
Quadratic bottom friction (c_D)	$[2.0 ; 3.0] \times 10^{-3}$	Dimensionless
Linear bottom friction (c_l)	$[1.5 ; 5.0] \times 10^{-4}$	m s^{-1}
Intensity factor (I)	[0.25 ; 1.25]	Dimensionless
Winddirection (Θ)	[-15 ; 15]	°
Runoff (Q)	$[8.0 ; 56.0] \times 10^{3}$	m^3 s^{-1}

Table 3. Statistical parameters and input values for the "optimal" simulation of the storm surge of May, 2000, for Palermo and Oyarvide.

		R	**P**	**RMSE (m)**	c_l	c_D	**I**	**Θ (°)**	**Q (m^3 s^{-1})**
NCEP/NCAAR - RI	**Palermo**	0,97	0,97	0,15	$1.5 \cdot 10^{-4}$	$2.1 \cdot 10^{-3}$	0.9	0,0	20,600
	Oyarvide	0,91	0,81	0,21					
ERA - INTERIM	**Palermo**	0,98	1,01	0,12	$2.2 \cdot 10^{-4}$	$2.1 \cdot 10^{-3}$	0.8	1.5	17,700
	Oyarvide	0,97	1,17	0,13					